Glial and neuronal isoforms of Neurofascin have distinct roles in the assembly of nodes of Ranvier in the central nervous system

Barbara Zonta,[1] Steven Tait,[1] Shona Melrose,[1] Heather Anderson,[1] Sheila Harroch,[2] Jennifer Higginson,[1] Diane L. Sherman,[1] and Peter J. Brophy[1]

[1]Centre for Neuroscience Research, Royal (Dick) School of Veterinary Studies, University of Edinburgh, Edinburgh EH9 1QH, Scotland, UK
[2]Département De Neuroscience, Institut Pasteur, 75 724 Paris, France

Rapid nerve impulse conduction in myelinated axons requires the concentration of voltage-gated sodium channels at nodes of Ranvier. Myelin-forming oligodendrocytes in the central nervous system (CNS) induce the clustering of sodium channels into nodal complexes flanked by paranodal axoglial junctions. However, the molecular mechanisms for nodal complex assembly in the CNS are unknown. Two isoforms of Neurofascin, neuronal Nfasc186 and glial Nfasc155, are components of the nodal and paranodal complexes, respectively. Neurofascin-null mice have disrupted nodal and paranodal complexes. We show that transgenic Nfasc186 can rescue the nodal complex when expressed in *Nfasc*$^{-/-}$ mice in the absence of the Nfasc155–Caspr–Contactin adhesion complex. Reconstitution of the axoglial adhesion complex by expressing transgenic Nfasc155 in oligodendrocytes also rescues the nodal complex independently of Nfasc186. Furthermore, the Nfasc155 adhesion complex has an additional function in promoting the migration of myelinating processes along CNS axons. We propose that glial and neuronal Neurofascins have distinct functions in the assembly of the CNS node of Ranvier.

Introduction

Nodes of Ranvier are the sites of action potential propagation in myelinated fibers, and their formation is essential for the switch to rapid nerve impulse transmission in the developing vertebrate nervous system. Axonal protein complexes containing voltage-gated sodium channels are assembled at nodes of Ranvier in response to myelination. In addition to sodium channels, components of the nodal complex include βIV-Spectrin, AnkyrinG, Contactin (in the central nervous system [CNS]), NrCAM (in the peripheral nervous system [PNS]), and a neuronal isoform of Neurofascin, Nfasc186 (Davis et al., 1996; Berghs et al., 2000; Tait et al., 2000; Jenkins and Bennett, 2002; Yang et al., 2004). The paranodal axoglial junctions that flank the node are formed by an adhesion complex between the glial isoform of Neurofascin, Nfasc155, and the axonal proteins Caspr (also known as Paranodin) and Contactin (Menegoz et al., 1997; Peles et al., 1997; Tait et al., 2000; Bhat et al., 2001; Boyle et al., 2001; Kazarinova-Noyes et al., 2001; Charles et al., 2002; Sherman and Brophy, 2005; Sherman et al., 2005). Axoglial junctions restrict the diffusion of nodal complexes but cannot cluster them in the PNS in the absence of Nfasc186 in vivo (Rios et al., 2003; Sherman et al., 2005).

Studies on myelinating cocultures have indicated a key role for nodal Nfasc186 in the clustering and stabilization of macromolecular assemblies at the PNS node of Ranvier (Lambert et al., 1997; Bennett and Lambert, 1999; Lustig et al., 2001; Koticha et al., 2006; Dzhashiashvili et al., 2007), and studies in vivo have supported this view (Sherman et al., 2005). Gliomedin, a protein expressed in the region of Schwann cell microvilli, may anchor Nfasc186 at the PNS node by virtue of its ability to interact with both Neurofascin and NrCAM (Eshed et al., 2005; Eshed et al., 2007; Maertens et al., 2007). However, there are indications that the mechanisms of node assembly may be different in the CNS. Soluble factors secreted by oligodendrocytes have been shown to promote sodium channel clustering in CNS axons in culture in the absence of axoglial contact (Kaplan et al., 1997). More recent work has refined this picture by showing that $Na_v1.2$ α subunits cluster under the influence of a secreted factor; however, clustering of $Na_v1.6$ α subunits, which are more characteristic of mature nodes, requires ensheathment by oligodendrocytes (Boiko et al., 2001;

Correspondence to Peter J. Brophy: Peter.Brophy@ed.ac.uk

Abbreviations used in this paper: CNS, central nervous system; MAG, myelin-associated glycoprotein; MBP, myelin basic protein; NF-L, neurofilament light chain; P, postnatal day; PNS, peripheral nervous system.

J. Cell Biol. Vol. 181 No. 7 1169–1177
www.jcb.org/cgi/doi/10.1083/jcb.200712154

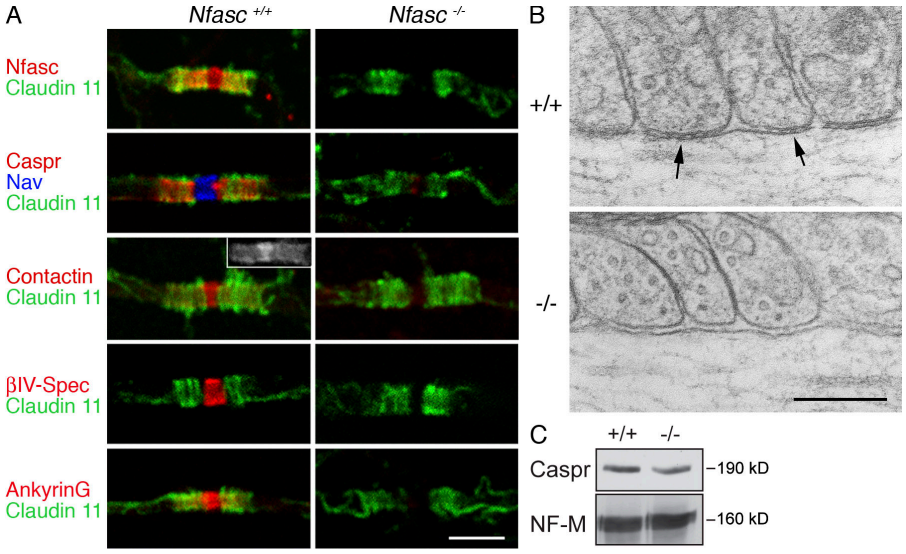

Figure 1. **Disruption of CNS paranodes and nodes in *Nfasc*$^{-/-}$ mice.** (A) Immunofluorescence analysis of teased fibers from the ventral funiculus of the cervical spinal cord from *Nfasc*$^{+/+}$ and *Nfasc*$^{-/-}$ animals showed that nodes and paranodes were disrupted when Nfasc155 and Nfasc186 were lost. Immunostaining of teased fibers for Claudin 11 (Oligodendrocyte-specific protein) was used to localize the paranodes of CNS myelin. Immunostaining with an antibody that recognized both Nfasc186 and Nfasc155 (Nfasc) confirmed that they were no longer at the node and paranode, respectively. The axoglial junctional components Caspr and Contactin were also no longer concentrated at the paranodes. In the CNS, Contactin is present at both the node and paranodes (inset). The nodal components voltage-gated sodium channels (Nav), Contactin, βIV-Spectrin (βIV-Spec), and AnkyrinG were mislocalized in mutant animals. Note that AnkyrinG in the CNS has both a nodal and paranodal localization. Bar, 5 µm. (B) Electron microscopy of the paranodes in wild-type (+/+) and mutant (−/−) mice. Septate junctions at the base of paranodal loops (arrows) were no longer present in the mutant. Bar, 0.2 µm. (C) Western blot analysis of cervical cord homogenates from wild-type (+/+) and *Nfasc*$^{-/-}$ (−/−) mice, respectively, showing that absence of the Neurofascins does not affect the amount of Caspr in the tissue. Neurofilament-M (NF-M) was used as a loading control.

Kaplan et al., 2001). These studies have further suggested that vesicular traffic is required to deliver sodium channels to nascent nodes (Kaplan et al., 2001).

Analysis of mice with mutations that affect the integrity of paranodal axoglial junctions has suggested that these structures, though not essential for the initial clustering of sodium channels, may be important for the long-term maintenance of the nodal complex (Bhat et al., 2001; Ishibashi et al., 2002; Rasband et al., 2003; Rios et al., 2003; Dupree et al., 2005). Derangement of the node after loss of axon–glial contact in tissue from multiple sclerosis patients caused by inflammatory damage to CNS axons is consistent with a role for the junction in stabilizing the node (Howell et al., 2006). However, thus far it has not been possible to discriminate between the relative contributions of nodal and paranodal Neurofascins in the initial assembly of the nodal complex in the CNS.

In this paper, we have studied how axonal and glial Neurofascins contribute to the clustering of sodium channels at CNS nodes of Ranvier in vivo by using *Nfasc*$^{-/-}$ mice with disrupted nodal and paranodal protein complexes. By selectively expressing either Nfasc186 or a truncated version of Nfasc155 by transgenesis in Neurofascin-null mice, we have been able to show that, in marked contrast to the PNS, each of the Neurofascin isoforms can independently rescue the CNS node of Ranvier. Furthermore, we have revealed an important function for the paranodal axoglial junction in promoting the migration and convergence of myelinating processes along axons. We propose that these two Neurofascin isoforms cooperate to assemble and maintain functional nodes of Ranvier in the vertebrate CNS.

Results

CNS phenotype of *Nfasc*$^{-/-}$ mice

Neurofascin-null animals die suddenly at 7 d after birth (Sherman et al., 2005). Therefore, analysis of their phenotype was performed at postnatal-day (P) 6. For most of this work, we used either teased fiber preparations or longitudinal sections from the ventral funiculus of the cervical spinal cord because we found that CNS myelination was most advanced there at this early stage of postnatal development in the mouse. Furthermore, this region of the spinal cord has relatively large axons, thus facilitating the preparation of teased fibers for microscopy and quantitation (Arroyo et al., 2002). Immunofluorescence showed that in Neurofascin-null nerves, there was extensive disruption to both the nodal complex (sodium channels, βIV-Spectrin, and AnkyrinG) and the paranodal axoglial junction (Caspr; Fig. 1 A). The paranodal myelin marker Claudin 11 was used to identify paranodes (and by inference nodes; Gow et al., 1999). Contactin was present at both the nodes and paranodes of wild-type nerves (Fig. 1 A, figure and inset), as previously reported (Kazarinova-Noyes et al., 2001) but was no longer detectable at either site in the mutant (Fig. 1 A). Similarly, AnkyrinG is not only a major component of the node of Ranvier, but it is also detectable at wild-type paranodes at this stage of CNS development (Rasband et al., 1999; Jenkins and Bennett, 2002); however, it is lost in the mutant in both locations (Fig. 1 A).

Disruption of the junctional complex at the paranode in the CNS was accompanied by loss of the characteristic septate junctions between the paranodal loops and the axolemma (Fig. 1 B). However, although it was mislocalized, there were normal amounts of Caspr in mutant spinal cord tissue, suggesting that disruption of the axoglial adhesion complex did not impair the biosynthesis and/or stability of the protein (Fig. 1 C).

Electron microscopy revealed myelinating and unmyelinated profiles in both wild-type and mutant nerves (Fig. 2 A). However, Western blotting showed that the levels of the myelin proteins myelin-associated glycoprotein (MAG) and myelin basic protein (MBP) in the CNS of the mutant at P6 were reduced compared with wild-type tissue and that they were similar to those observed at P4 in the wild-type (Fig. 2 B). This suggested

that myelination might be either retarded or halted in the mutant. The reduction in myelin protein in the mutant was accompanied by a significant decrease in the number of myelinated axons observed at P6 in the ventral funiculus of the mutant cervical spinal cord (Fig. 2 C). The reduction in the amount of myelin was not a consequence of a general decrease in the number of axons in the CNS of Neurofascin-null animals because the total number of axons in the optic nerves of mutants was normal (Fig. 2 D). Neither was the reduced extent of myelination a consequence of an inadequate pool of myelin-forming glia because the numbers of oligodendrocytes in wild-type and mutant cervical spinal cord sections were not significantly different (Fig. 2 E).

Nfasc186 rescues the nodal complex

We used a transgenic approach to ask if expression of Nfasc186 FLAG tagged at its C terminus could reconstitute the nodal complex in the CNS axons of *Nfasc*$^{-/-}$ mice in vivo in the absence of an intact axoglial adhesion complex. First, it was important to demonstrate that this epitope-tagged protein was targeted appropriately to the node of Ranvier and that it colocalized with the nodal complex (sodium channels, βIV-Spectrin, Contactin, and AnkyrinG) in *Nfasc*$^{+/+}$ mice (Fig. 3 A). Then, we showed that expression of transgenic Nfasc186 on a Neurofascin-null background was fully able to rescue the nodal complex (Fig. 3 A). Intriguingly, and in contrast to Contactin, AnkyrinG in the rescued fibers resumed its normal localization at both the node and paranode (Fig. 3 A). This suggests that the transient expression of AnkyrinG at the paranodes during the postnatal development of myelinated CNS fibers does not depend on either Nfasc155 or its axonal partners Caspr and Contactin because in the absence of Nfasc155, there was no amelioration of the mislocalization of Caspr (Fig. 3 B). The transient nature of paranodal AnkyrinG is shown by its loss in both wild-type and Nfasc186-rescued nerves by P16 (Fig. 3 D).

Importantly, the nodal rescue by Nfasc186 was functionally significant because these mice survived beyond P7 only to succumb at P18–19. This allowed us to study two developmentally regulated events in myelinated CNS axons, namely, the expression of juxtaparanodal potassium channels and the upregulation of sodium channels of the Nav1.6 type. Absence of an intact axoglial junction caused juxtaparanodal potassium channels of the *Shaker* type Kv1.1 to redistribute to ectopic sites close to the nodal sodium channels, as has been observed in other mutants with deranged axoglial junctions (Fig. 3 B; Bhat et al., 2001; Boyle et al., 2001). However, the developmentally regulated switch to sodium channels of the Nav1.6 type was unimpaired by the absence of an axoglial junction (Fig. 3 C) as was found in the *Jimpy* mouse (Jenkins and Bennett, 2002).

We have shown previously that a form of Nfasc155 with most of the C terminus replaced by a FLAG tag (Nfasc155ΔIC) is targeted to the paranodal loops of myelinating Schwann cells and oligodendrocytes (Sherman et al., 2005). Further, we showed that it can reconstitute the axoglial junctional complex in the peripheral nerves of Neurofascin-null mice (Sherman et al., 2005), presumably by virtue of the ability of the extracellular domain to interact with components of the axonal Caspr–Contactin complex (Charles et al., 2002; Gollan et al., 2003). However, these

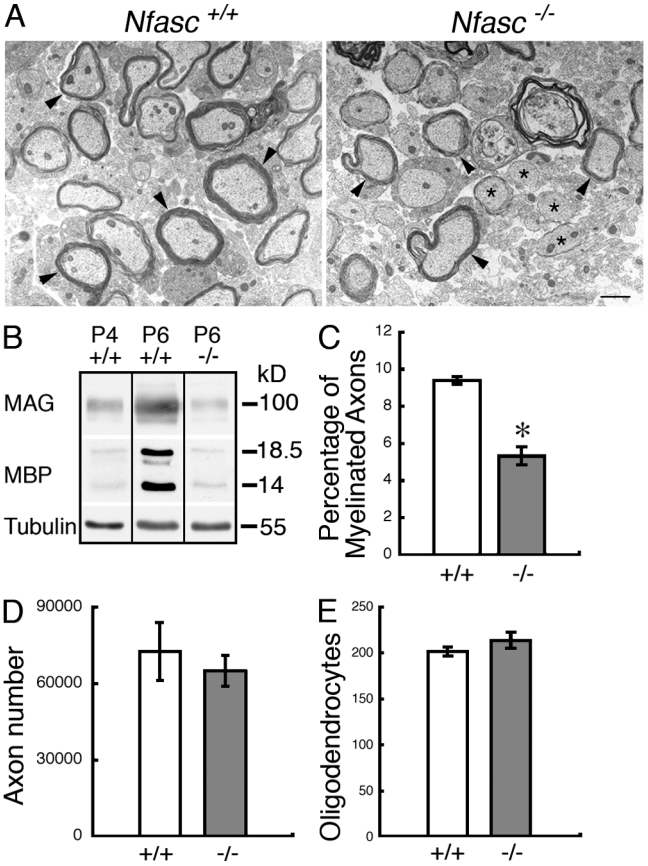

Figure 2. **Reduced myelination in the mutant at P6.** (A) Electron microscopy of transverse sections from the cervical cord of 6-d-old *Nfasc*$^{+/+}$ and *Nfasc*$^{-/-}$ animals showed that, at this very early stage of CNS myelination, both myelinating (arrowheads) and nonmyelinated (asterisks) profiles were visible in wild-type and mutant cord. Bar, 1 µm. (B) Western blot analysis of cervical cord homogenates from wild-type and *Nfasc*$^{-/-}$ mice showed that the myelin components MAG and MBP were reduced in the mutant at P6 and were comparable to the levels found at P4 in the wild type. Tubulin was the loading control. All the blots were from the same gel and the exposures were identical for each protein. (C) The percentage of myelinated axons in cervical cord sections was reduced in the mutant. (D) The total number of axons in the optic nerves of wild-type and mutant nerves was not significantly different. (E) Oligodendrocyte numbers in wild-type and mutant spinal cord cross sections were not significantly different. Values are means ± SEM. $n = 3$ mice for each condition. *, $P < 0.01$ (unpaired Student's *t* test).

reconstituted paranodal complexes could not rescue sodium channels in the absence of Nfasc186 at PNS nodes (Sherman et al., 2005). Using the neuron-specific *neurofilament light chain* (*NF-L*) promoter, *Nfasc186* transgenic mice also displayed robust expression in the PNS, which allowed us to show directly in vivo that Nfasc186 could rescue the nodal complex (sodium channels, βIV-Spectrin, AnkyrinG, and NrCAM) in the absence of an intact axoglial junction in PNS axons (Fig. 4 A). Interestingly, we were also able to show that NrCAM is a component of PNS nodes but that it is absent from CNS nodes (Fig. 4 B).

Reconstitution of the axoglial adhesion complex rescues CNS nodal sodium channels

Although reconstitution of the axoglial junction cannot rescue the nodal complex in the PNS in the absence of Nfasc186, we wished to ask if the same holds true in the CNS. Nfasc155ΔIC

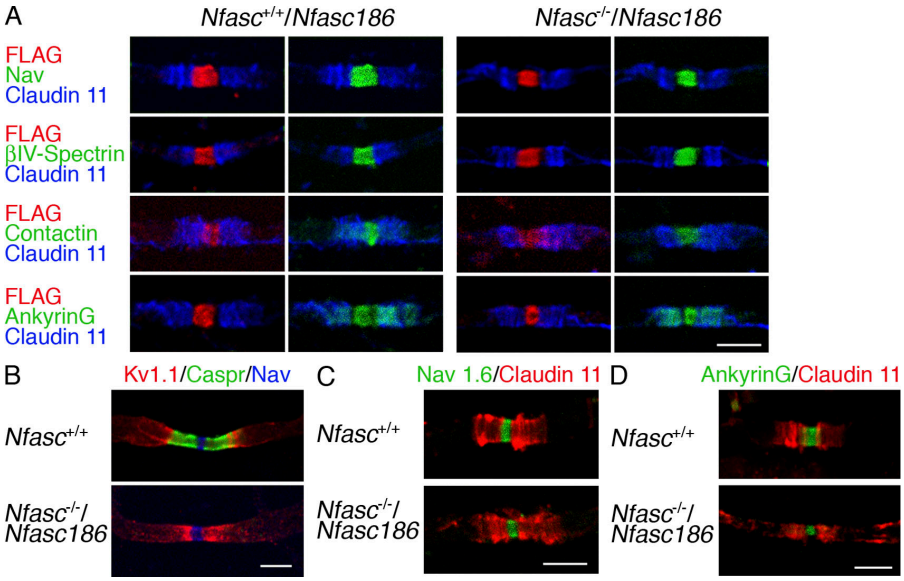

Figure 3. **Nfasc186 rescues the CNS nodal complex in *Nfasc*$^{-/-}$ mice.** (A) Immunostaining of teased ventral funiculus fibers in the CNS at P6 shows that FLAG-tagged Nfasc186 is targeted to the nodes of myelinated axons and that it can rescue the nodal components, voltage-gated sodium channels (Nav), βIV-Spectrin, Contactin, and AnkyrinG when expressed on a Neurofascin-null background. Immunostaining of teased fibers for the paranodal myelin marker Claudin 11 was used to confirm the localization of the node of Ranvier. Note that nodal rescue of AnkyrinG also retrieved the protein to the paranodes. (B) Immunostaining for Caspr at P16 showed that reconstitution of the nodal complex by expressing FLAG-tagged Nfasc186 on a Neurofascin-null background was not accompanied by rescue of the axoglial junction and that, as a consequence, juxtaparanodal Kv1.1 channels were mislocalized. (C) By P16, CNS nodes contain Nav1.6 channels, indicating that the absence of the axoglial junction does not prevent developmental changes in the expression of sodium channel subtypes. (D) By P16 AnkyrinG is concentrated at the nodes and lost at the paranodes in wild-type and *Nfasc*$^{-/-}$ nerves rescued with Nfasc186. Bars, 5 µm.

reconstituted the paranodal axoglial adhesion complex in the CNS of *Nfasc*$^{-/-}$ mice (Fig. 5 A), but, in complete contrast to the PNS, the correct localization of nodal sodium channels was also rescued (Fig. 5 B). Other components of the CNS nodal complex, such as βIV-Spectrin, were also correctly localized (Fig. 5 B). Unlike the Nfasc186 rescue, mice expressing Nfasc155ΔIC on a Neurofascin-null background did not have an enhanced life expectancy. This may be because of the fact that nodal complexes in the PNS are not rescued concomitantly with those in the CNS.

Nodal gaps of less than 5 µm in width were identified by symmetrical Claudin 11 immunostaining, and the percentage of these that were immunostained for sodium channels was measured. In wild-type axons of the spinal cord ventral funiculus, 100% of such nodal gaps immunostained for sodium channels (Fig. 5 C). The efficiency of sodium channel rescue was equally high when reconstituting the axoglial junction with Nfasc155ΔIC or when expressing Nfasc186 (91 ± 4 and 96 ± 2%, respectively; mean ± SEM; n = 3 each; Fig. 5 C). In both cases, there was no significant difference in the frequency of sodium channel staining when compared with wild-type nodes (Fig. 5 C).

Interestingly, it was possible to detect sodium channels at a minority of Claudin 11–flanked nodes in Neurofascin-null nerves (16.0 ± 6.1%; mean ± SEM; n = 3; Fig. 5 C). This suggested that sodium channels could still be targeted to the node in *Nfasc*$^{-/-}$ mice but that the efficiency of their delivery and/or their stability upon arrival was impaired in the absence of Nfasc186 or an intact axoglial junction. The ability of the Nfasc155–Caspr–Contactin adhesion complex to promote the concentration of voltage-gated sodium channels at CNS nodes in the absence of Nfasc186 is in marked contrast to the PNS node (Sherman et al., 2005), and this difference was confirmed in this paper using a transgene encoding the complete Nfasc155 protein (Fig. 5 D).

The Nfasc155-Caspr-Contactin adhesion complex promotes oligodendrocyte process migration

The distal extremities of oligodendrocyte processes in teased preparations of wild-type nerves immunostained strongly for glial Nfasc155 together with its axonal partners in the axoglial adhesion complex Caspr (Fig. 6, A and B) and Contactin (not depicted). This was so not only when the myelinating processes had converged to form a nascent paranodal complex at P6 (Fig. 6 B) but also when they were still migrating and the interheminodal gap was >14 µm apart, as was observed frequently at P4 (Fig. 6 A). Oligodendrocyte processes also migrated along axons in *Nfasc*$^{-/-}$ and *Nfasc*$^{-/-}$*/Nfasc186* mice (Fig. 6, C and D). However, quantitative analysis showed that the convergence of heminodes was significantly impaired at P6 in Neurofascin-null nerves and was not ameliorated by the presence of nodal Nfasc186 (Fig. 6 F). This retardation of oligodendrocyte process migration appeared to be a consequence of the absence of an intact axoglial junction because the interheminodal gap between processes in wild-type mice at an earlier stage of development (P4; 31.7 ± 3.9 µm; mean ± SEM; n = 3) were not statistically different from either *Nfasc*$^{-/-}$ or *Nfasc*$^{-/-}$*/Nfasc186* mice at P6 (32.5 ± 33.4 and 39.1 ± 3.5 µm, respectively; mean ± SEM; n = 3 each [analysis of variance]).

At P6 in wild-type axons, 75% of the nodes were <5 µm in length, whereas in the mutant lacking both Neurofascins at the same age the equivalent number was 17%, which further underlined the reduction in process convergence in the absence of Nfasc155 and an intact axoglial junction. The fact that there was no statistical difference between the interheminodal gap in wild-type CNS axons compared with Neurofascin-null nerves rescued with the *Nfasc155ΔIC* transgene underlined the ability of Nfasc155 to promote normal process migration through restoration of the axoglial junction (Fig. 6, E and F).

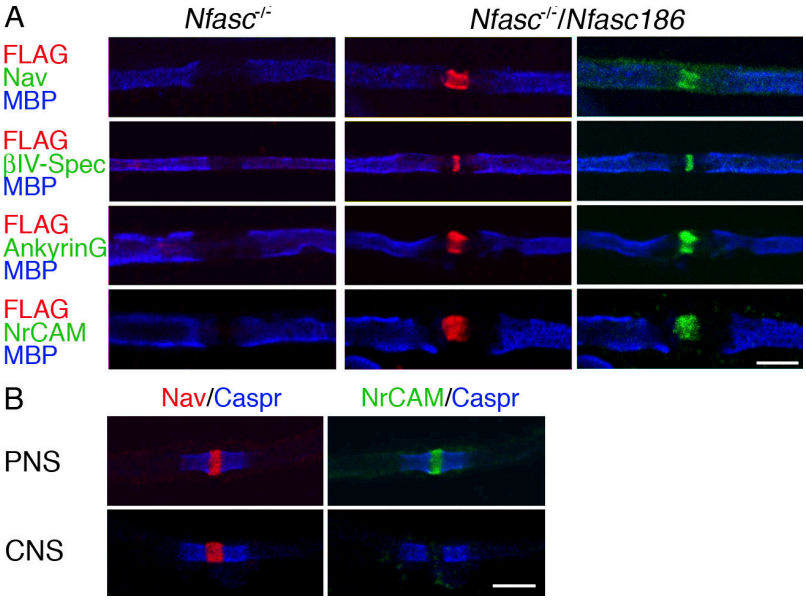

Figure 4. **Nfasc186 rescues the PNS nodal complex in *Nfasc*$^{-/-}$ mice.** (A) FLAG-tagged Nfasc186 can rescue the nodal complex in teased sciatic nerve fibers immunostained for the nodal proteins voltage-gated sodium channels (Nav), βIV-Spectrin, AnkyrinG, and NrCAM. Myelin was visualized using MBP as a marker. (B) NrCAM is present at PNS nodes but absent from CNS nodes. Bars, 5 μm.

Neurofascin-null mice rescued with the *Nfasc186* transgene had an extended lifespan, and this allowed us to ask whether oligodendrocyte process migration was either delayed or was completely stalled in the absence of Nfasc155 at P6. In contrast to P6 (Fig. 6 F), at P16 there was no significant difference in the interheminodal gap between *Nfasc*$^{+/+}$ and *Nfasc*$^{-/-}$*/Nfasc186* mice (Fig. 6 G). Hence, the absence of an axoglial adhesion complex delayed, rather than prevented, the extension and convergence of oligodendrocyte processes altogether, and electron microscopy showed that this delay did not cause dysmyelination (Fig. 6 H).

Discussion

The mechanisms of assembly of the node of Ranvier and the clustering of sodium channels are likely to occur by different mechanisms in the CNS when compared with the PNS, not least because of the different structure and protein composition of their nodal environments (Kaplan et al., 1997, 2001; Poliak and Peles, 2003; Salzer, 2003; Sherman and Brophy, 2005). For example, Contactin is a characteristic component of CNS nodes but is absent from PNS nodes, whereas we find that the reverse is true for NrCAM (Kazarinova-Noyes et al., 2001).

Previous work has provided strong circumstantial evidence that the axoglial junction might have a role in the formation of the CNS node. Analysis of the developing optic nerve showed that Caspr staining, which is indicative of the formation of axoglial complexes, preceded the detection of sodium channel clusters, which were initially typically broad (Rasband et al., 1999). The same authors showed that *Shiverer* mutant mice lacking normal axoglial junctions had reduced and ectopic sodium channel clusters. This indicated, probably for the first time, that there was a relationship between the integrity of the axoglial junctional complex and the ability of myelinated CNS axons to cluster sodium channels. Subsequent analysis of another mutant, UDP-galactose/ceramide galactosyltransferase–deficient mice, which also lacks intact paranodal axoglial junctions, showed that it was able to form Nav1.6 channel clusters at nodes but that these became more diffuse and less concentrated with time (Rasband et al., 2003). Interestingly, Contactin and Caspr were still detectable in paranodal complexes in these mice, whereas Nfasc155 was not (Schafer et al., 2004). These observations may be reconciled by our demonstration here that either Nfasc186 or Nfasc155 (through the formation of the axoglial complex) can promote the assembly of the nodal complex. Thus, in the case of the ceramide galactosyltransferase mutant mice, Nfasc186 delivered to the axolemma, possibly guided by local concentrations of Caspr and Contactin, might drive the assembly of the node in the absence of the paranodal junction.

The tips of oligodendrocyte processes visualized in the teased fiber preparations used in the present work are enriched in Nfasc155 and Caspr. The early formation of axoglial junctions has been observed previously in the optic nerve, and it is known that axoglial septate junctions can be detected in the same nerve as early as after one turn of the myelinating process around an axon (Wiggins et al., 1988; Rasband et al., 1999). The fact that process migration is retarded in the absence of these proteins suggests that the axoglial adhesion complex has a role in promoting their extension. Nevertheless, the ability of the processes to ultimately converge shows that the axoglial complex is not solely responsible for allowing oligodendrocyte processes to extend. Recent evidence for the involvement of the WAVE proteins and their associated links with the actin cytoskeleton in oligodendrocyte process extension provides a possible additional mechanism (Kim et al., 2006).

Signaling via the axoglial adhesion complex might stimulate oligodendrocytes to extend their myelinating processes. However, Nfasc155 lacking most of its C terminus can not only reconstitute the adhesion complex but can also cluster nodal proteins, which shows that intracellular signaling mediated via the carboxy terminus of Nfasc155 is not necessary to promote the assembly of the node of Ranvier in the CNS. This raises the intriguing idea that intracellular signaling in the axon in response to axoglial interaction, possibly mediated by the cytoplasmic

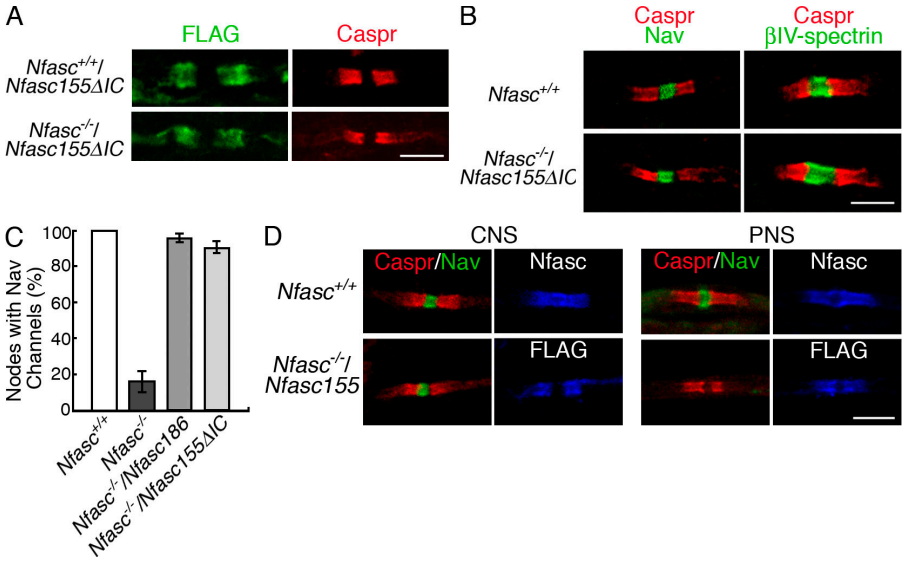

Figure 5. **Reformation of the paranodal adhesion complex rescues the node.** (A) Immunostaining of longitudinal sections of the spinal cord ventral funiculus in the CNS shows that FLAG-tagged Nfasc155ΔIC is targeted to the paranodes of myelinated axons and that it can rescue Caspr to the paranodal axoglial junctional complex in *Nfasc*$^{-/-}$ mice. (B) Rescue of Caspr to the paranode by Nfasc155ΔIC on a Neurofascin-null background reconstitutes voltage-gated sodium channels (Nav) and βIV-Spectrin to the nodal complex. (C) In the CNS at P6, both Nfasc186 and Nfasc155ΔIC are equally effective at reconstituting nodes with sodium channels (Nav) when expressed in the absence of endogenous Neurofascins. The percentage of nodal gaps of <5 µm in width identified by Claudin 11 immunostaining that also had sodium channels was measured. (D) Full-length Nfasc155 tagged with FLAG at the C terminus reconstitutes the axoglial junction in both CNS and PNS, but nodal Nav channels are only rescued in the CNS. Neurofascins were detected in the wild type using a pan anti-Neurofascin antibody that recognizes both Nfasc155 and Nfasc186. Values are means ± SEM. *n* = 3 mice for each condition. Bars, 5 µm.

tail of Caspr, may stimulate the extension of oligodendrocyte processes during myelination, in addition to the role of the oligodendrocyte actin cytoskeleton and the WAVE proteins. Certainly, and unlike Nfasc155, Caspr cannot contribute to stable axoglial junctions without its intracellular domain (Gollan et al., 2002). Further, a short sequence in this domain mediates binding to the cytoskeleton-associated protein 4.1B, which is itself part of a cytoskeletal complex that includes AnkyrinB (Gollan et al., 2002; Ogawa et al., 2006). Interestingly, most mice lacking AnkyrinB die at P8, although some survive until P21 and have a particularly severe phenotype in the CNS where optic nerves degenerate (Scotland et al., 1998). This may reflect defects in axon-glia signaling.

The role of the axoglial adhesion complex in the extension of oligodendrocyte processes most probably accounts for the reduced extent of myelination in the CNS of Neurofascin-null mice at P6. This is in contrast to the PNS, where myelination is unaffected at P6 in the absence of the Neurofascins (Sherman et al., 2005). The cell biology of myelination by oligodendrocytes when compared with that of Schwann cells may underlie these differences. Oligodendrocyte processes must first extend from their cell bodies, make contact with axons, and then extend along them to completely ensheath internodes. In contrast, Schwann cells in vivo cover the axons that they are destined to ensheath before myelination ensues (Jessen and Mirsky, 2005). Hence, the sites of nascent nodes of Ranvier are already defined by where each Schwann cell abuts its neighbors. The mechanisms by which Schwann cells subsequently grow and elongate are not fully understood but appear to involve the cytoplasm-filled Cajal bands, which are uniquely Schwann cell structures (Court et al., 2004).

The internodes of CNS axons are up to three times shorter than those in the PNS at a given axon diameter. Nevertheless, the CNS node of Ranvier still accounts for <1% of the length of the adjacent internode (Ramon y Cajal, 1909; Fraher, 1978). In spite of the fact that nodes constitute such short segments of the axon, clustered sodium channels are still detectable at ∼16% of nascent nodes in *Nfasc*$^{-/-}$ nerves. This indicates that sodium channels are not randomly delivered to the axolemma but are targeted to the nascent node independently of either Nfasc186 or Nfasc155, although one or both of these proteins is clearly required to stabilize the nascent node. Interestingly, a previous study found that ∼12% of sodium channel clusters in the developing optic nerve was not associated with Caspr-positive axoglial junctions (Rasband et al., 1999). However, these clusters would be expected to contain Nfasc186, which, as the present work shows, would be sufficient to promote the assembly of the nodal complex.

Sodium channels are probably delivered to the nascent node via an exocytotic pathway (Kaplan et al., 2001). It has been proposed that AnkyrinG might regulate such targeting (Jenkins and Bennett, 2002); however, this still leaves the question open as to how AnkyrinG is itself delivered to the nascent node. Once the sodium channels with their associated β subunits reach the nodal membrane, they would be expected to interact with Nfasc186 and βIV-Spectrin to form a macromolecular complex (Ratcliffe et al., 2001; McEwen and Isom, 2004). In the absence of Nfasc186, the complex would diffuse in the lateral plane of the membrane, and without an intact axoglial junction to function as a sieve or barrier to their further dispersal, the nodal proteins may be endocytosed or proteolyzed in the internodal region, as occurs in the PNS (Pedraza et al., 2001; Dzhashiashvili et al., 2007). Reintroduction of Nfasc186 would reduce the dissipation of the complex by anchoring it at the node. Because sodium channels, their β subunits, and AnkyrinG can interact with Nfasc186 directly, their presence at the node could also drive the targeted delivery of Nfasc186 (Ratcliffe et al., 2001; Jenkins and Bennett, 2002; McEwen and Isom, 2004).

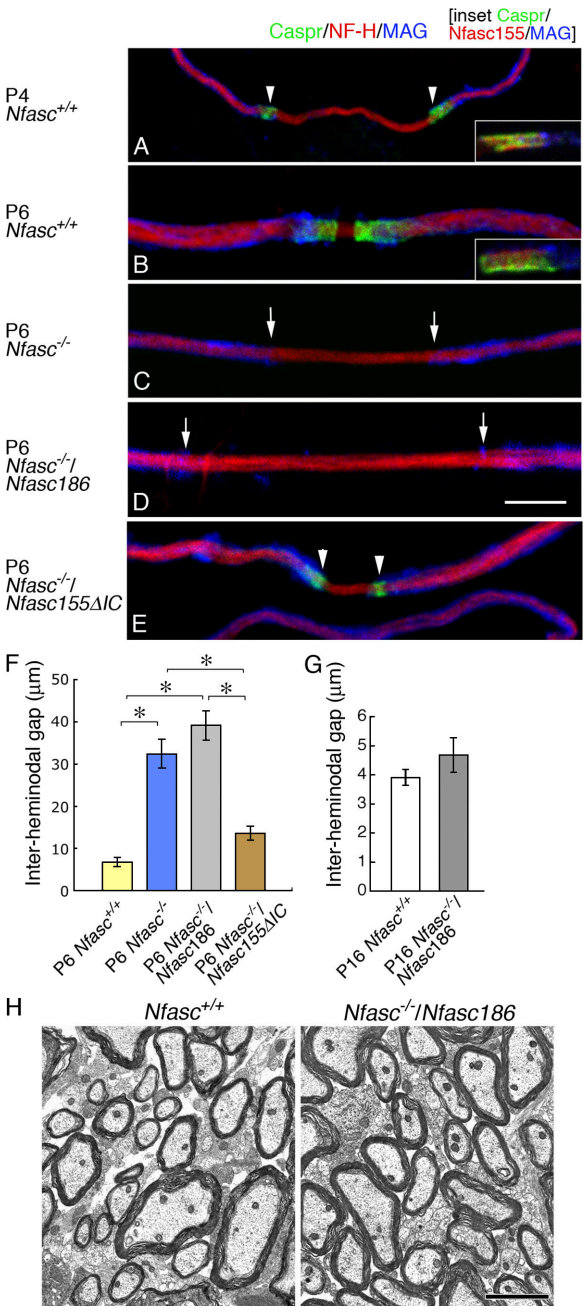

Figure 6. **Axoglial adhesion complex promotes oligodendrocyte process migration.** (A and B) Axoglial adhesion complexes at the tips of myelinating processes in teased fibers were immunostained for Caspr or Caspr and Nfasc155 (insets) at P4 (A) and P6 (B). Immunostaining for the myelin protein MAG, the axonal marker NF-H, Caspr, and Nfasc155 suggested that oligodendrocyte processes with Neurofascin and Caspr at their tips might converge from P4 to P6 during development. (C–E) Myelinating processes could extend along axons in *Nfasc*$^{-/-}$ mice (C) and in Neurofascin-null mice expressing either Nfasc186 (D) or C-terminally truncated Nfasc155 (E). (F) Measurement of the gap between myelinating processes (the interheminodal gap) at P6 showed that the convergence of oligodendrocyte processes in teased fibers from the ventral funiculus of the cervical spinal cord is either retarded or stalled in the mutant, with or without Nfasc186, compared with wild-type nerves at the same age. There was no significant difference in the mean interheminodal gap of mutant fibers at P6 with or without Nfasc186, but each was significantly larger than the nodal width in either wild-type nerves at P6 or when the axoglial adhesion complex was reconstituted using C-terminally truncated Nfasc155. However, there was no significant difference in the width of the gap in wild-type nerves compared with Neurofascin-null nerves rescued with C-terminally truncated Nfasc155, indicating that this protein effectively rescued process migration. (G) At P16, the interheminodal gap between myelinating processes in nerves from cervical spinal cord lacking an intact axoglial junction is not significantly different from wild type, showing that convergence of myelinating processes is retarded rather than arrested at P6. Values are means ± SEM. $n = 3$ mice for each condition. *, $P < 0.01$ (one-way analysis of variance test). (H) Electron microscopy of transverse sections from the cervical cord of 16-d old *Nfasc*$^{+/+}$ and *Nfasc*$^{-/-}$*/Nfasc186* animals showed extensive myelination in the rescued mutant cord. In A and E, the arrowheads show the position of the adhesion complex. In C and D, the arrows show the tips of oligodendrocyte processes. Bars: (A–E) 5 μm; (H) 2 μm.

The clustering of sodium channels can occur independently of the presence of an intact axoglial junction. Nevertheless, there is a tendency for nodal sodium channels to disperse over time when the paranodal junctional complex is disrupted (Rios et al., 2003). The importance of an intact axoglial junction for the long-term stability of the nodal complex has also been demonstrated in mouse mutants and after chemical disruption of the myelin sheath (Ishibashi et al., 2002; Dupree et al., 2005). The limited extension of viability in Neurofascin-null mice expressing transgenic Nfasc186 may reflect their lack of intact axoglial junctions because Caspr-null mice lacking paranodal junctions in the CNS and PNS generally die between P21 and P33 (Bhat et al., 2001). Interestingly, the tendency for the nodal complex to become more diffuse is more pronounced in the CNS compared with the PNS (Rios et al., 2003). This suggests that the junctional complex plays a more important role in containing the nodal complex in the CNS than in the PNS, which is consistent with a more prominent role for the axoglial junction in assembling the CNS nodal complex.

An intriguing question is why CNS nodes exploit two distinct mechanisms to concentrate the macromolecular complex required for saltatory conduction at the node of Ranvier, whereas in the PNS, Nfasc186 has a uniquely important role. The role of Nfasc186 in the PNS had been inferred from previous experiments both in vivo and in vitro (Sherman et al., 2005; Dzhashiashvili et al., 2007), and here we have demonstrated its absolute requirement in PNS node assembly in vivo. Once anchored at the PNS node via extracellular interactions, possibly mediated by gliomedin and intracellular association with the actin cytoskeleton by means of AnkyrinG and βIV-Spectrin, Nfasc186 participates in an exceptionally stable complex, as indicated by the relative insensitivity of sodium channels to dispersion after disruption of the paranodal axoglial junction (Bhat et al., 2001; Boyle et al., 2001; Rios et al., 2003). The uniquely PNS nodal component, NrCAM, may also play a part here because it is known to interact with Nfasc186 (Volkmer et al., 1996). In the absence of NrCAM, CNS nodes may depend on the axoglial junction to provide an independent mechanism for focusing and concentrating sodium channels to complement their cis interactions with Nfasc186. Future application of the transgenic rescue strategy described in this work should allow us to functionally dissect the protein–protein interactions by which Nfasc186 and Nfasc155 cooperate in the assembly of the CNS node of Ranvier.

Materials and methods

Animals

All animal work conformed to UK legislation (Scientific Procedures) Act 1986 and to the University of Edinburgh Ethical Review Committee policy. The generation of *Nfasc*$^{-/-}$ and transgenic mice, *Nfasc155ΔIC*, expressing a truncated form of Nfasc155 under the control of the *Plp* promoter has been previously described (Sherman et al., 2005). Transgenic mice, *NFasc155*, expressing the full-length Nfasc155 with a FLAG tag at its C terminus under the control of the *Plp* promoter, were generated as for the *Nfasc155ΔIC* line. Transgenic mice expressing a full-length cDNA encoding Nfasc186 under the control of the *NF-L* promoter *Nfasc186* were similarly generated by pronuclear injection. After introducing a FLAG tag sequence at the 3′ of the coding region, the cDNA was cloned into the ClaI site of the pGCHNF-L vector (J.-P. Julien [Laval University, Quebec City, Canada] and D.E. Merry [Thomas Jefferson University, Philadelphia, PA]) and was released using AscI and NotI. After backcrossing to a C57BL/6 background, one of the lines was interbred with *Nfasc*$^{+/-}$ mice to generate *Nfasc*$^{-/-}$*/Nfasc186* mice.

Antibodies, microscopy, and Western blots

Unless indicated otherwise, all microscopic images were from nerves of 6-d-old animals. For immunostaining of CNS or PNS teased fiber preparations at room temperature, the ventral funiculus of the cervical spinal cord or sciatic nerves, respectively, were removed after transcardiac perfusion with 4% PFA and 0.1 M sodium phosphate buffer, pH 7.4, fixed for a further 30 min in 4% PFA and 0.1 M sodium phosphate buffer, pH 7.4, washed in several changes of phosphate buffer, and teased on 3-aminopropyltriethoxysilane–coated slides. A rabbit anti-Contactin antibody was prepared using Contactin fused to the Fc domain of human IgG that had been expressed in 293 cells and purified from the medium using protein A–sepharose (1:200). Other primary antibodies were used at the following dilutions: rabbit NFC1 (pan anti-Nfasc; Tait et al., 2000), 1:2,000; rabbit NFF3 (anti–third fibronectin type III domain of Nfasc155; Tait et al., 2000), 1:2,000; rabbit anti-FLAG (Sigma-Aldrich), 1:400; mouse anti-FLAG (Sigma-Aldrich), 1:250; guinea pig anti-Caspr (D.R. Colman, Montreal Neurological Institute, Montreal, Canada), 1:200; mouse anti-Caspr (IgM; M. Rasband, Baylor College of Medicine, Houston, TX), 1:50; rabbit anti-MBP (Vouyiouki is and Brophy, 1993), 1:1,000; rabbit anti–βIII tubulin (Sigma-Aldrich), 1:2,000; rabbit anti-Nav1.6 (M. Rasband), 1:100; chicken anti-MBP (Millipore), 1:50; rabbit anti-NrCAM (Sherman et al., 2005), 1:200; rabbit anti-MAG (Charles et al., 2002), 1:500; chicken anti–βIV-Spectrin (Komada and Soriano, 2002; M. Komada, Tokyo Institute of Technology, Yokohama, Japan), 1:200; rabbit anti-AnkyrinG (V. Bennett, Duke University, Durham, NC), 1:5,000; mouse pan anti–sodium channel (IgG1; Sigma-Aldrich), 1:200; rabbit anti–Claudin 11 (Invitrogen), 1:100; mouse anti–Claudin 11 (A. Gow, Wayne State University, Detroit, MI), 1:100; mouse anti-APC (IgG2; EMD), 1:100; mouse anti–Neurofilament-H (IgG1; Sigma-Aldrich), 1:200; and mouse anti–Neurofilament-M (IgG1; Sigma-Aldrich), 1:2,000. The secondary antibodies were used at the following dilutions: goat FITC-conjugated anti–rabbit IgG (Cappel), 1:200; donkey FITC-conjugated anti–chicken IgY (Jackson ImmunoResearch Laboratories), 1:200; donkey TRITC-conjugated anti–guinea pig IgG (Jackson ImmunoResearch Laboratories), 1:200; donkey FITC-conjugated anti–mouse IgM (Jackson ImmunoResearch Laboratories), 1:200; goat TRITC-conjugated anti–mouse IgG1 (SouthernBiotech), 1:200; and goat Alexa Fluor 647–conjugated anti–mouse IgG1 (Invitrogen), 1:200. Samples were mounted in Vectashield (Vector Laboratories). For confocal microscopy, we used a confocal microscope (TCL-SL; Leica) with a 1.4 NA 63× objective and Leica proprietary software. Conventional fluorescence microscopy was performed using a microscope (BX60; Olympus) and a 0.75 NA 40× objective lens, and images were captured using a camera (Orca-ER; Hamamatsu Photonics) and Openlab software (Improvision). Interheminodal gaps were measured using Openlab software after image acquisition using conventional fluorescence microscopy. The same system was used to measure the total number of spinal cord oligodendrocytes in transverse sections after immunostaining with an anti-APC antibody (five sections per animal, three animals per condition). Nerves were prepared for electron microscopy as described previously (Gillespie et al., 2000). To compare the percentages of myelinated fibers in wild-type and mutant spinal cord, 10 random images from three animals were captured at a magnification of 65K and the fraction of axons with a diameter ≥0.5 µm surrounded by myelin was measured. The total number of axons in an optic nerve was determined by measuring the axonal density in five regions of interest of 140 µm^2 per nerve using three animals at a magnification of 65K and relating this to the total area of the optic nerve using Openlab software. Electron microscopic images were captured using a Biotwin (Phillips) either by conventional photography or by using a digital camera (Orius; Gatan). Photographic negatives were scanned and digitized. All figures were prepared using Photoshop version 7.0 (Adobe) and were not subjected to any subsequent image processing. Western blotting was performed as previously described (Sherman et al., 2005).

We thank S. Fleming, B. Smith, and E. Scholefield for technical support and R. Johnson for assistance in constructing the transgene used to generate mice expressing Nfasc155. Generous gifts of antibodies from Drs. V. Bennett, D.R. Colman, A. Gow, M. Komada, and M. Rasband and the pGCHNF-L vector from Drs J.-P. Julien and D.E. Merry are gratefully acknowledged.

This work was supported by the Medical Research Council and the Wellcome Trust.

Submitted: 27 December 2007
Accepted: 29 May 2008

References

Arroyo, E.J., T. Xu, J. Grinspan, S. Lambert, S.R. Levinson, P.J. Brophy, E. Peles, and S.S. Scherer. 2002. Genetic dysmyelination alters the molecular architecture of the nodal region. *J. Neurosci.* 22:1726–1737.

Bennett, V., and S. Lambert. 1999. Physiological roles of axonal ankyrins in survival of premyelinated axons and localization of voltage-gated sodium channels. *J. Neurocytol.* 28:303–318.

Berghs, S., D. Aggujaro, R. Dirkx Jr., E. Maksimova, P. Stabach, J.M. Hermel, J.P. Zhang, W. Philbrick, V. Slepnev, T. Ort, and M. Solimena. 2000. βIV spectrin, a new spectrin localized at axon initial segments and nodes of Ranvier in the central and peripheral nervous system. *J. Cell Biol.* 151:985–1002.

Bhat, M.A., J.C. Rios, Y. Lu, G.P. Garcia-Fresco, W. Ching, M. St Martin, J. Li, S. Einheber, M. Chesler, J. Rosenbluth, et al. 2001. Axon-glia interactions and the domain organization of myelinated axons requires neurexin IV/Caspr/Paranodin. *Neuron.* 30:369–383.

Boiko, T., M.N. Rasband, S.R. Levinson, J.H. Caldwell, G. Mandel, J.S. Trimmer, and G. Matthews. 2001. Compact myelin dictates the differential targeting of two sodium channel isoforms in the same axon. *Neuron.* 30:91–104.

Boyle, M.E., E.O. Berglund, K.K. Murai, L. Weber, E. Peles, and B. Ranscht. 2001. Contactin orchestrates assembly of the septate-like junctions at the paranode in myelinated peripheral nerve. *Neuron.* 30:385–397.

Charles, P., S. Tait, C. Faivre-Sarrailh, G. Barbin, F. Gunn-Moore, N. Denisenko-Nehrbass, A.M. Guennoc, J.A. Girault, P.J. Brophy, and C. Lubetzki. 2002. Neurofascin is a glial receptor for the paranodin/Caspr-contactin axonal complex at the axoglial junction. *Curr. Biol.* 12:217–220.

Court, F.A., D.L. Sherman, T. Pratt, E.M. Garry, R.R. Ribchester, D.F. Cottrell, S.M. Fleetwood-Walker, and P.J. Brophy. 2004. Restricted growth of Schwann cells lacking Cajal bands slows conduction in myelinated nerves. *Nature.* 431:191–195.

Davis, J.Q., S. Lambert, and V. Bennett. 1996. Molecular composition of the node of Ranvier: identification of ankyrin-binding cell adhesion molecules neurofascin (mucin+/third FNIII domain−) and NrCAM at nodal axon segments. *J. Cell Biol.* 135:1355–1367.

Dupree, J.L., J.L. Mason, J.R. Marcus, M. Stull, R. Levinson, G.K. Matsushima, and B. Popko. 2005. Oligodendrocytes assist in the maintenance of sodium channel clusters independent of the myelin sheath. *Neuron Glia Biol.* 1:1–14.

Dzhashiashvili, Y., Y. Zhang, J. Galinska, I. Lam, M. Grumet, and J.L. Salzer. 2007. Nodes of Ranvier and axon initial segments are ankyrin G–dependent domains that assemble by distinct mechanisms. *J. Cell Biol.* 177:857–870.

Eshed, Y., K. Feinberg, S. Poliak, H. Sabanay, O. Sarig-Nadir, I. Spiegel, J.R. Bermingham Jr., and E. Peles. 2005. Gliomedin mediates Schwann cell-axon interaction and the molecular assembly of the nodes of Ranvier. *Neuron.* 47:215–229.

Eshed, Y., K. Feinberg, D.J. Carey, and E. Peles. 2007. Secreted gliomedin is a perinodal matrix component of peripheral nerves. *J. Cell Biol.* 177:551–562.

Fraher, J.P. 1978. Quantitative studies on the maturation of central and peripheral parts of individual ventral motoneuron axons. II. Internodal length. *J. Anat.* 127:1–15.

Gillespie, C.S., D.L. Sherman, S.M. Fleetwood-Walker, D.F. Cottrell, S. Tait, E.M. Garry, V.C. Wallace, J. Ure, I.R. Griffiths, A. Smith, and P.J. Brophy. 2000. Peripheral demyelination and neuropathic pain behavior in periaxin-deficient mice. *Neuron.* 26:523–531.

Gollan, L., H. Sabanay, S. Poliak, E.O. Berglund, B. Ranscht, and E. Peles. 2002. Retention of a cell adhesion complex at the paranodal junction requires the cytoplasmic region of Caspr. *J. Cell Biol.* 157:1247–1256.

Gollan, L., D. Salomon, J.L. Salzer, and E. Peles. 2003. Caspr regulates the processing of contactin and inhibits its binding to neurofascin. *J. Cell Biol.* 163:1213–1218.

Gow, A., C.M. Southwood, J.S. Li, M. Pariali, G.P. Riordan, S.E. Brodie, J. Danias, J.M. Bronstein, B. Kachar, and R.A. Lazzarini. 1999. CNS myelin and sertoli cell tight junction strands are absent in Osp/claudin-11 null mice. *Cell.* 99:649–659.

Howell, O.W., A. Palser, A. Polito, S. Melrose, B. Zonta, C. Scheiermann, A.J. Vora, P.J. Brophy, and R. Reynolds. 2006. Disruption of neurofascin localization reveals early changes preceding demyelination and remyelination in multiple sclerosis. *Brain.* 129:3173–3185.

Ishibashi, T., J.L. Dupree, K. Ikenaka, Y. Hirahara, K. Honke, E. Peles, B. Popko, K. Suzuki, H. Nishino, and H. Baba. 2002. A myelin galactolipid, sulfatide, is essential for maintenance of ion channels on myelinated axon but not essential for initial cluster formation. *J. Neurosci.* 22:6507–6514.

Jenkins, S.M., and V. Bennett. 2002. Developing nodes of Ranvier are defined by ankyrin-G clustering and are independent of paranodal axoglial adhesion. *Proc. Natl. Acad. Sci. USA.* 99:2303–2308.

Jessen, K.R., and R. Mirsky. 2005. The origin and development of glial cells in peripheral nerves. *Nat. Rev. Neurosci.* 6:671–682.

Kaplan, M.R., A. Meyer-Franke, S. Lambert, V. Bennett, I.D. Duncan, S.R. Levinson, and B.A. Barres. 1997. Induction of sodium channel clustering by oligodendrocytes. *Nature.* 386:724–728.

Kaplan, M.R., M.H. Cho, E.M. Ullian, L.L. Isom, S.R. Levinson, and B.A. Barres. 2001. Differential control of clustering of the sodium channels Na(v)1.2 and Na(v)1.6 at developing CNS nodes of Ranvier. *Neuron.* 30:105–119.

Kazarinova-Noyes, K., J.D. Malhotra, D.P. McEwen, L.N. Mattei, E.O. Berglund, B. Ranscht, S.R. Levinson, M. Schachner, P. Shrager, L.L. Isom, and Z.C. Xiao. 2001. Contactin associates with Na+ channels and increases their functional expression. *J. Neurosci.* 21:7517–7525.

Kim, H.J., A.B. DiBernardo, J.A. Sloane, M.N. Rasband, D. Solomon, B. Kosaras, S.P. Kwak, and T.K. Vartanian. 2006. WAVE1 is required for oligodendrocyte morphogenesis and normal CNS myelination. *J. Neurosci.* 26:5849–5859.

Komada, M., and P. Soriano. 2002. βIV-spectrin regulates sodium channel clustering through ankyrin-G at axon initial segments and nodes of Ranvier. *J. Cell Biol.* 156:337–348.

Koticha, D., P. Maurel, G. Zanazzi, N. Kane-Goldsmith, S. Basak, J. Babiarz, J. Salzer, and M. Grumet. 2006. Neurofascin interactions play a critical role in clustering sodium channels, ankyrin G and beta IV spectrin at peripheral nodes of Ranvier. *Dev. Biol.* 293:1–12.

Lambert, S., J.Q. Davis, and V. Bennett. 1997. Morphogenesis of the node of Ranvier: co-clusters of ankyrin and ankyrin-binding integral proteins define early developmental intermediates. *J. Neurosci.* 17:7025–7036.

Lustig, M., G. Zanazzi, T. Sakurai, C. Blanco, S.R. Levinson, S. Lambert, M. Grumet, and J.L. Salzer. 2001. Nr-CAM and neurofascin interactions regulate ankyrin G and sodium channel clustering at the node of Ranvier. *Curr. Biol.* 11:1864–1869.

Maertens, B., D. Hopkins, C.W. Franzke, D.R. Keene, L. Bruckner-Tuderman, D.S. Greenspan, and M. Koch. 2007. Cleavage and oligomerization of gliomedin, a transmembrane collagen required for node of Ranvier formation. *J. Biol. Chem.* 282:10647–10659.

McEwen, D.P., and L.L. Isom. 2004. Heterophilic interactions of sodium channel beta1 subunits with axonal and glial cell adhesion molecules. *J. Biol. Chem.* 279:52744–52752.

Menegoz, M., P. Gaspar, M. Le Bert, T. Galvez, F. Burgaya, C. Palfrey, P. Ezan, F. Arnos, and J.A. Girault. 1997. Paranodin, a glycoprotein of neuronal paranodal membranes. *Neuron.* 19:319–331.

Ogawa, Y., D.P. Schafer, I. Horresh, V. Bar, K. Hales, Y. Yang, K. Susuki, E. Peles, M.C. Stankewich, and M.N. Rasband. 2006. Spectrins and ankyrinB constitute a specialized paranodal cytoskeleton. *J. Neurosci.* 26:5230–5239.

Pedraza, L., J.K. Huang, and D.R. Colman. 2001. Organizing principles of the axoglial apparatus. *Neuron.* 30:335–344.

Peles, E., M. Nativ, M. Lustig, M. Grumet, J. Schilling, R. Martinez, G.D. Plowman, and J. Schlessinger. 1997. Identification of a novel contactin-associated transmembrane receptor with multiple domains implicated in protein-protein interactions. *EMBO J.* 16:978–988.

Poliak, S., and E. Peles. 2003. The local differentiation of myelinated axons at nodes of Ranvier. *Nat. Rev. Neurosci.* 4:968–980.

Ramon y Cajal, S. 1909. Histologie du Systeme Nerveux de l'Homme et des Vertebris. Vol. 1. Maloine, Paris. 986 pp.

Rasband, M.N., E. Peles, J.S. Trimmer, S.R. Levinson, S.E. Lux, and P. Shrager. 1999. Dependence of nodal sodium channel clustering on paranodal axoglial contact in the developing CNS. *J. Neurosci.* 19:7516–7528.

Rasband, M.N., C.M. Taylor, and R. Bansal. 2003. Paranodal transverse bands are required for maintenance but not initiation of Nav1.6 sodium channel clustering in CNS optic nerve axons. *Glia.* 44:173–182.

Ratcliffe, C.F., R.E. Westenbroek, R. Curtis, and W.A. Catterall. 2001. Sodium channel β1 and β3 subunits associate with neurofascin through their extracellular immunoglobulin-like domain. *J. Cell Biol.* 154:427–434.

Rios, J.C., M. Rubin, M. St Martin, R.T. Downey, S. Einheber, J. Rosenbluth, S.R. Levinson, M. Bhat, and J.L. Salzer. 2003. Paranodal interactions regulate expression of sodium channel subtypes and provide a diffusion barrier for the node of Ranvier. *J. Neurosci.* 23:7001–7011.

Salzer, J.L. 2003. Polarized domains of myelinated axons. *Neuron.* 40:297–318.

Schafer, D.P., R. Bansal, K.L. Hedstrom, S.E. Pfeiffer, and M.N. Rasband. 2004. Does paranode formation and maintenance require partitioning of neurofascin 155 into lipid rafts? *J. Neurosci.* 24:3176–3185.

Scotland, P., D. Zhou, H. Benveniste, and V. Bennett. 1998. Nervous system defects of $Ankyrin_B$ (−/−) mice suggest functional overlap between the cell adhesion molecule L1 and 440-kD $Ankyrin_B$ in premyelinated axons. *J. Cell Biol.* 143:1305–1315.

Sherman, D.L., and P.J. Brophy. 2005. Mechanisms of axon ensheathment and myelin growth. *Nat. Rev. Neurosci.* 6:683–690.

Sherman, D.L., S. Tait, S. Melrose, R. Johnson, B. Zonta, F.A. Court, W.B. Macklin, S. Meek, A.J. Smith, D.F. Cottrell, and P.J. Brophy. 2005. Neurofascins are required to establish axonal domains for saltatory conduction. *Neuron.* 48:737–742.

Tait, S., F. Gunn-Moore, J.M. Collinson, J. Huang, C. Lubetzki, L. Pedraza, D.L. Sherman, D.R. Colman, and P.J. Brophy. 2000. An oligodendrocyte cell adhesion molecule at the site of assembly of the paranodal axo-glial junction. *J. Cell Biol.* 150:657–666.

Volkmer, H., R. Leuschner, U. Zacharias, and F.G. Rathjen. 1996. Neurofascin induces neurites by heterophilic interactions with axonal NrCAM while NrCAM requires F11 on the axonal surface to extend neurites. *J. Cell Biol.* 135:1059–1069.

Vouyioukiis, D.A., and P.J. Brophy. 1993. Microtubule-associated protein MAP1B expression precedes the morphological differentiation of oligodendrocytes. *J. Neurosci. Res.* 35:257–267.

Wiggins, R.C., G. Chongjie, C. Delaney, and T. Samorajski. 1988. Development of axonal-oligodendroglial relationships and junctions during myelination of the optic nerve. *Int. J. Dev. Neurosci.* 6:233–243.

Yang, Y., S. Lacas-Gervais, D.K. Morest, M. Solimena, and M.N. Rasband. 2004. BetaIV spectrins are essential for membrane stability and the molecular organization of nodes of Ranvier. *J. Neurosci.* 24:7230–7240.